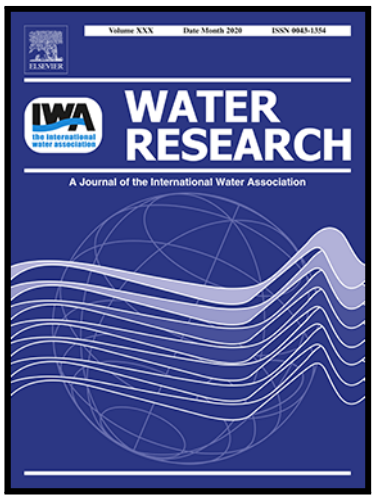

Mechanisms of high ammonium loading promoted phosphorus release from shallow lake sediments: a five-year large-scale experiment

Shuo-Nan Ma , Yuan-Feng Xu , Hai-Jun Wang , Hong-Zhu Wang , Yan Li , Xu-Meng Dong , Ji-Lin Xu , Qing Yu , Martin Søndergaard , Erik Jeppesen

PII: S0043-1354(23)01020-5
DOI: https://doi.org/10.1016/j.watres.2023.120580
Reference: WR 120580

To appear in: *Water Research*

Received date: 27 May 2023
Revised date: 25 August 2023
Accepted date: 4 September 2023

Please cite this article as: Shuo-Nan Ma , Yuan-Feng Xu , Hai-Jun Wang , Hong-Zhu Wang , Yan Li , Xu-Meng Dong , Ji-Lin Xu , Qing Yu , Martin Søndergaard , Erik Jeppesen , Mechanisms of high ammonium loading promoted phosphorus release from shallow lake sediments: a five-year large-scale experiment, *Water Research* (2023), doi: https://doi.org/10.1016/j.watres.2023.120580

Highlights

- N-induced P release was most pronounced in summer and from sediment rich in organic matter
- Sediment acidification by long-term N application partly explained the P release
- A positive feedback loop of "P-algae-fish" was found
- In this loop, algae-stimulated fish-biomass increased disturbance, promoting P release

Mechanisms of high ammonium loading promoted phosphorus release from shallow lake sediments: a five-year large-scale experiment

Shuo-Nan Ma[a, b], Yuan-Feng Xu [b], Hai-Jun Wang*[a, c], Hong-Zhu Wang*[a], Yan Li[a], Xu-Meng Dong [b], Ji-Lin Xu [b], Qing Yu[a], Martin Søndergaard[d, e], Erik Jeppesen[c, d, e, f, g]

[a] State Key Laboratory of Freshwater Ecology and Biotechnology, Institute of Hydrobiology, Chinese Academy of Sciences, Wuhan 430072, China

[b] School of Marine Sciences, Ningbo University, Ningbo 315832, China

[c] Institute for Ecological Research and Pollution Control of Plateau Lakes, School of Ecology and Environmental Science, Yunnan University, Kunming, China

[d] Department of Ecoscience and WATEC, Aarhus University, Aarhus 8000, Denmark

[e] Sino-Danish Centre for Education and Research (SDC), University of Chinese Academy of Sciences, Beijing 100190, China

[f] Limnology Laboratory, Department of Biological Sciences and Centre for Ecosystem Research and implementation, Middle East Technical University, Ankara 06800, Turkey

[g] Institute of Marine Sciences, Middle East Technical University, 33731 Erdemli-Mersin, Turkey

E-mail Addresses of Authors:

Shuo-Nan Ma: mashuonan@nbu.edu.cn;
Yuan-Feng Xu: 1901130057@nbu.edu.cn;
Hai-Jun Wang: wanghaijun@ynu.edu.cn;
Hong-Zhu Wang: wanghz@ihb.ac.cn;
Yan Li: liyan@ihb.ac.cn;
Xu-Meng Dong: xumengd@gmail.com;
Ji-Lin Xu: xujilin@nbu.edu.cn;
Qing Yu: yuqzoe@163.com;
Martin Søndergaard: ms@ecos.au.dk;
Erik Jeppesen: ej@ecos.au.dk.

*Corresponding author: 7 South Donghu Road, Wuchang District, Wuhan 430072, P.

R. China. Tel.: + 86 27 68780225; fax: +86 27 68780064.

Abstract

The unprecedented global increase in the anthropogenic-derived nitrogen (N) input may have profound effects on phosphorus (P) dynamics and may potentially lead to enhanced eutrophication as demonstrated in short-term mesocosm experiments. However, the role of N-influenced P release is less well studied in large-scale ecosystems. To gain more insight into ecosystem effects, we conducted a five-year large-scale experiment in ten ponds (700 – 1000 m^2 each) with two types of sediments and five targeted total N concentrations (TN) by adding NH_4Cl fertilizer (0.5, 1, 5, 10, and 25 mg N L^{-1}). The results showed that: i) The sediment P release increased significantly when TN exceeded 10 – 25 mg N L^{-1}. ii) The most pronounced sediment P release increase occurred in summer and from sediments rich in organic matter (OM_{Sed}). iii) TN, algal biomass, fish biomass, non-algal turbidity, sediment pH, and OM_{Sed} were the dominant factors explaining the sediment P release, as suggested by piecewise structural equation modeling. We propose several mechanisms that may have stimulated P release, i.e. high ammonium input causes a stoichiometric N:P imbalance and induce alkaline phosphatase production and dissolved P uptake by phytoplankton, leading to enhanced inorganic P diffusion gradient between sediment and water; higher pelagic fish production induced by the higher phytoplankton production may have led increased sediment P resuspension through disturbance; low oxygen level in the upper sediment caused by nitrification and organic decomposition of the settled phytoplankton and, finally, long-term N application-induced sediment acidification as a net effect of ammonium hydrolysis, nitrification, denitrification; The mechanisms revealed by this study shed new light on the complex processes underlying the N-stimulated sediment P release, with implications also for the strategies used for restoring eutrophicated lakes.

Key words: Eutrophication; Nitrogen pollution, Internal phosphorus loading, Bioturbation, Sediment acidification

1. Introduction

Global anthropogenic nitrogen (N) and phosphorus (P) inputs to the biosphere have increased asymmetrically since the late 1980s due to intensive human activities (Wu et al., 2022). The imbalanced inputs of N and P have significantly increased the N/P ratio (Peñuelas & Sardans, 2022) and resulted in pervasive high N concentrations in lakes (Gruber & Galloway, 2008; Yu et al., 2019). More specifically, N concentrations in water bodies were low before the 1980s in China (typically <1.0 mg L^{-1}) but increased rapidly to a high level, exceeding 5 – 10 mg L^{-1} in lakes at some places in the 1990s (Yu et al., 2019; Liu et al., 2019). Besides negatively affecting water quality, biodiversity, and human health (Peñuelas et al., 2020), high N inputs to aquatic ecosystems may profoundly influence the internal P loading, which acts as a bottleneck in restoring lake water quality (Søndergaard et al., 2003; Jeppesen et al., 2005). For example, mesocosm experiments (150 – 1000 L in volume) have suggested that, once the ammonium (NH_4^+) concentration reaches approximately 10 mg N L^{-1}, alkaline phosphatase activity (APA) might be stimulated and hence promote sediment P release (Ma et al., 2018). Low nitrate (NO_3^-) addition (1.2 – 2.2 mg N L^{-1}) has been used as an oxidant with hindering effects on the sediment P release in some stratified lakes during periods of hypolimnetic anoxia (Ripl, 1976; Søndergaard et al., 2000); while high NO_3^- levels exceeding 5 – 10 mg N L^{-1} may have a dual effect, inhibiting the sediment P release by improving the redox potential while promoting the P release by increasing the biomass of phytoplankton at the same time (Ma et al., 2021). The coupled N and P cycle would add fuel to water eutrophication by enhancing the bioavailable P. However, studies on the effects of N input on P dynamics have mainly been conducted at a small scale and with limited temporal resolution, while long-term large-scale studies are generally absent.

Although previous mesocosm tests have largely revealed how N loading impacts the sediment P release, the involved mechanisms may have been too coarse as some

features of lakes (e.g., wide-ranging organisms and their disturbance, natural mixing regime, and heterogeneity of sediment characteristics) play vital roles in P dynamics but are usually not well included in mesocosm systems (Schindler, 1998; Huser et al., 2016). Specifically, fish can contribute to the P transport from sediment to water through sediment disturbance when foraging (Tarvainen et al., 2005; Huser et al., 2016), but their natural behavior cannot easily be mimicked in mesocosms. Mesocosms also typically lack a natural mixing regime, which may hamper the penetration of O_2 from air to bottom water (Schindler, 1998), favoring anoxic-desorption release of P (Jiang et al., 2008; Ma et al., 2018). However, whether such a mechanism is also active in shallow lakes with mixed and aerated water needs to be further elucidated. Sediment characteristics, in particular organic matter (OM) contents, often vary greatly between lakes and within specific lakes, leading to different oxygen demands and P behaviors such as adsorption-desorption, migration, and transformation (Liu et al., 2009; Li et al., 2016; Deng et al., 2022).

Furthermore, the short duration (less than one season) of the mesocosm experiments does not allow researchers to accurately assess the response of slow-responding organisms and biogeochemical processes (Schindler, 1998). For example, fish at the top of the food chains in natural lakes required at least several years to respond fully to nutrient addition (Meijer et al., 1994; Schindler, 1998). pH is another important determinant of the fate of P dynamics (Cooke et al., 2005). At pH ≤ 6, the soluble forms of aluminum and calcium compounds dominate, and P desorption and activation proceed (Cooke et al., 2005). Although sediment pH may decrease after NH_4^+ addition (a net effect of NH_4^+ hydrolysis, nitrification, and denitrification) (Hao et al., 2020; Wang et al., 2022), it typically occurs under long-term N application, suggesting that pH-related mechanisms in sediment have little to work at short-term scales (Zeng et al., 2017; Hao et al., 2020).

Overall, the pivotal role of spatial and temporal scales in ecosystem experiments is underappreciated, yet critical for lake P dynamics. Thus, long-term and large-scale experiments are needed to calibrate and verify that smaller-scale experiments properly represent the interplay of ecosystem-scale processes to an extent where the results can

be extrapolated with confidence to ecosystem-scale issues. We hypothesize that high N loading will contribute to the P release by increasing the extent of anoxia, sediment acidification, and fish disturbance (N-stimulated algal growth may increase fish biomass by acting as food) at a long-term ecosystem scale. To test this hypothesis, we conducted a five-year whole-ecosystem experiment in ten ponds with two substrate types and a gradient of NH_4^+ loading.

2. Materials and methods

2.1. Study area and experimental system set-up

The experiment was carried out at the Lake Bao'an Field Station of Experimental Limnological Research, which is part of the Aquatic Mesocosm Facilities in Asia (http://mesocosm.org/facilities/). Lake Bao'an is a meso-eutrophic lake (area: 48 km^2; mean water depth: 1.9 m) located on the south bank of the middle Yangtze River. This region experiences four distinct seasons and has a warm, humid subtropical climate with a mean annual precipitation of 1552 mm and a mean air temperature of 18 ℃ (Fig. S1). Modified from a lotus pond, our experimental pond (N 30˚17′17″, E 114˚43′45″) was dredged to remove nutrients, e.g., N, P, and organic matter (OM), in the surface 20 cm sediments before being divided into 10 parts (area: 700 – 1000 m^2 each; mean depth: 1.6 m) by embankment construction (Fig. S2, Fig. 1). Two types of sediment (clay rich in OM and loam poor in OM) were collected from the surface 10 cm sediments of Lake Bao'an and subsequently added to two groups of ponds (five ponds in each group) to obtain a sediment layer of 10 cm. The remaining 1.5 m was filled with unfiltered water from Lake Bao'an using a pump. The ten ponds were then grouped into two clearly separated categories: high OM ponds (clayish in texture and with an OM between 17.3 and 33.6 g kg^{-1} dw, coded as Sed_{High}) and low OM ponds (loamy in texture and with an OM between 1.5 and 9.4 g kg^{-1} dw, coded as Sed_{Low}) (Table 1, Fig. S3). The physico-chemical properties presented in Table 1 revealed that the sediments were moderately alkaline (pH ≥ 7.6) and had high P concentrations. Aiming at creating an experimental system close to natural systems, three cyprinids commonly appearing in shallow lakes and ponds along the mid-lower Yangtze Basin

(silver carp *Hypophthalmichthys molitrix Val.*, bighead carp *Aristichthys nobilis Richardson*, and gibel carp *Carassius auratus gibelio Bloch*) were introduced into the ponds from May to July, 2011. The fish were grouped into planktivorous fish (including silver carp and bighead carp, coded as $Fish_{Pla}$) and benthic fish (gibel carp, $Fish_{Ben}$) based on their feeding habits (Wang et al., 2017). All fish were obtained from the same commercial fish farm. Fifty silver carp (body weight: 0.6 ± 0.02 g (mean ± SE); body length: 0.8 ±0.06 cm), 20 bighead carp (body weight: 260 ± 5 g; body length: 26.7 ± 1.2 cm), and 100 gibel carp (body weight: 0.8 ±0.07 g; body length: 1.2 ± 0.07 cm) were randomly selected and transferred to each pond. The experiment began on August 13th, 2011 (three months after the sediment and water introduction) and ended on May 27th, 2016.

2.2. Experimental design

A gradient of five target TN concentrations was set in both the Sed_{Low} and Sed_{High} ponds: control without N addition (coded as $N_{0.5}$), 1 mg N g L^{-1} (N_1), 2 mg N L^{-1} (N_2), 10 mg N L^{-1} (N_{10}), and 25 mg N L^{-1} (N_{25}). N was added in the form of NH_4Cl (NH_4Cl, > 99.5%, Sinopharm Chemical Reagent Co., Ltd., Shanghai, China). NH_4^+ concentration of 0.5 mg N L^{-1} ($N_{0.5}$) refers to the background TN concentration as well as water quality Class Π as defined in the environmental quality standards for surface water in China (GB 3838-2002); NH_4^+ concentration of 1 mg N L^{-1} (N_1) refers to water quality Class Ш as defined in the environmental quality standards for surface water in China (GB 3838-2002); NH_4^+ concentrations of 5 mg N L^{-1} and 25 mg N L^{-1} (N_5 and N_{25}) refer to primary A and Class Π in the discharge standard of pollutants for municipal wastewater treatment plants in China (GB-18918-2002). During the whole experiment (from August, 2011 to May, 2016), the treatment ponds were enriched with NH_4Cl fertilizer at biweekly to monthly intervals with a dosage calculated from the target concentrations and the measured concentrations:

$$F = (T - M) * V \ldots\ldots\ldots\ldots\ldots\ldots\ldots\ldots\ldots Eq1$$

where T is the target TN concentration (mg N L^{-1}), M is the measured TN concentration (mg N L^{-1}), and V is the volume of pond water (L). To quickly achieve

high TN concentrations, nearly four times the target dose of N fertilizer were added in the first year. The amounts of NH_4Cl fertilizer added during the whole experimental period are shown in Fig. 2A. No external sources of P were introduced during the experiment.

2.3. Sampling and measurement

Depth-integrated water samples were taken approximately from the top to 10 cm above the sediment biweekly or monthly at five randomly chosen locations within each pond using a tube sampler (diameter: 10 cm, height: 1.5 m) and then pooled into one sample. One liter of well-mixed water was taken back to the laboratory within two hours for analyses of total nitrogen (TN), NH_4^+, NO_3^-, total phosphorus (TP), total turbidity ($Turb_{Tot}$), and phytoplankton chlorophyll *a* (Chl *a*) according to Ma et al. (2018). Another liter of water was immediately fixed with Lugol's solution (3%–5% final concentration) for phytoplankton analysis. Taxa were counted in sedimentation chambers (Hydro-Bios Apparatebau GmbH Kiel, Germany) with an inverted microscope (CK2, Olympus Corporation, Tokyo, Japan). B_{Phyt} (mg L^{-1}) was calculated as follows (Li et al., 2017):

$$B_{Phyt} = \sum_{i=1}^{S} \rho * V_i * D_i \ldots\ldots\ldots\ldots\ldots\ldots\ldots\ldots\ldots Eq2$$

Here, *S* is the taxa number of phytoplankton, ρ is phytoplankton density in mg·μm^{-3}, V_i is the biovolume of taxa *i* in μm^{-3}, and D_i is the density of taxa *i* in cells L^{-1}.

Water temperature (Temp), dissolved oxygen (DO), redox potential (Eh), and water pH at middle water depth were measured *in situ* during sampling using a YSI ProPlus (Yellow Spring Inc., USA). Secchi disk transparency (SD) and water depth (ZM) were determined *in situ* with a transparency disc and sounding lead, respectively. Additionally, high-frequency monitoring (2-day intervals) of TP, phosphate (PO_4^{3-}), Chl *a*, DO, pH, and alkaline phosphatase activity in sediment (APA) was carried out in ponds $N_{0.5a}$, N_{5a}, and N_{25a} from July 10th to July 26th, 2015.

Five sediment cores (with 5 cm surface sediment) were collected seasonally

(four times per year) at five random locations in each pond using a gravity coring device. Subsequently, the cores were pooled into one sample and homogenized for analyses of sediment texture (particle size), nutrient content (TN and P fractions), sediment OM (OM_{Sed}), APA, and sediment pH (pH_{Sed}). The particle size of the sediment was determined by the pipette method (Wang et al., 2005a) and categorized into three fractions: clay (<0.002 mm), silt (0.002 – 0.05 mm), and sand (0.05 – 2 mm). Given that the prevalent Psenner-type extraction is unsuitable for the analysis of P fractions in Ca^{2+} rich sediment because high Ca^{2+} may interfere with the extractant (sodium bicarbonate-conjugated sodium dithionite), leading to errors in the extraction of water-soluble P (Petterson et al.,1988; Psenner et al.,1984), thus we selected the Golterman extraction to determine the P fractions in our Ca^{2+}-rich (40 mg L^{-1}) case (Golterman, 1996). Sediment P was divided into different fractions such as iron-bound P (Fe_P), calcium-bound P (Ca_P), acid-soluble organic P (HCl_P), and hot NaOH-extractable organic P (NaOH_P) according to Golterman (1996). In detail, 1.5 g fresh sediment was extracted twice with 30 mL of 0.05 M Ca-EDTA for 2 h, 30 mL of 0.1 M Na_2-EDTA for 17 h, 30 mL of 0.5 M H_2SO_4 for 30 min, and 30 mL of 2 M NaOH at 90 °C for 30 min for successive extraction of Fe_P, Ca_P, HCl_P, and NaOH_P, respectively [organic P (Org_P) = HCl_P + NaOH_P]. The concentrations of extracted phosphate were measured according to the molybdate blue method (Ma et al., 2018). APA was determined according to the method of Abad-Valle et al. (2015). This method is based on analysis of released p-Nitrophenol (p-NP) after incubation of moist soil samples with p-Nitrophenyl disodium orthophosphate (p-NPP) at 37 ℃ for 1 h. Then 5 mL of 0.5 M NaOH was added to terminate the reaction. After centrifugation (3500 rpm, 15 min), supernatant was measured at 410 nm. pH_{Sed} was measured with a soil pH meter (pH 400&pH 600, USA). The diffusive technique gradients in thin films (DGT) were used for *in situ* measurement of Fe(Π) and labile-P (termed as easily changeable or mobile P fractions, including PO_4^{3-} and forms of P loosely adsorbed to sediment solids). DGT probes were forced 8 cm into the sediment and kept 2 cm above the water surface on July 12th, 14th, 17th, 22nd, and 26th, 2015 using a releasing device. After 48 hours, the probes were retrieved and brought to the

laboratory for determination of one-dimensional distributions of labile-P and Fe(Π) concentrations according to Ma et al. (2018).

Recapture of fish from each pond was done twice with a trawl net (mesh size: 15 mm) on November 7th, 2013. The recapture time for each pond was approximately 1.5 hours. All captured fish were counted, after which body length was measured with a measuring board and weighed with an electronic balance (0.01 g, BL-2200H, Shimadzu Corporation, Japan).

2.4. Data processing

Data on ten ponds were grouped into two categories for comparison: high OM ponds (Sed_{High}) and low OM ponds (Sed_{Low}). We used the response ratio (RR) and the log of the response ratio (L_{RR}) to determine the effect size of the N addition on the measured sediment P release because they equally weigh the negative and positive responses and facilitate statistical analysis (Marklein & Houlton, 2012). RR was calculated as the experimental values of TP divided by the simultaneously measured control values ($N_{0.5a}$ or $N_{0.5b}$), representing an index of response magnitudes; L_{RR} was calculated as the $\log_{10}$ of RR. Positive values of L_{RR} represent increased TP in the N treatment relative to the control, whereas negative values indicate inhibited P release.

To determine the relative contribution of planktonic algae and non-algal particles to turbidity, we used the method of Portielje and Van der Molen (1999) and divided $Turb_{Tot}$ (1/SD) into three parts: algal turbidity ($Turb_{Alg}$), non-algal turbidity ($Turb_{NonAlg}$), and background turbidity ($Turb_{Bck}$) in the absence of suspended particles. According to this method, $1/SD_{max}$ (the minimum value of 1/SD) is set as $Turb_{Bck}$ (planktonic algae and non-algal suspended particulate are assumed to be absent), and $Turb_{Bck}$ in our data set was 0.56 m^{-1}. The relation between transparency and Chl *a* can be formulated as Eq3 (Portielje & Van der Molen, 1999):

$$\frac{1}{SD} = \frac{1}{SD_0} + \left(\frac{\alpha}{PA}\right) Chl\ a \ldots\ldots\ldots\ldots\ldots\ldots\ldots\ldots\ldots Eq3$$

where SD_0 is the Secchi disk transparency in the absence of phytoplankton, α is the specific extinction coefficient of Chl *a* (m^2 g^{-1}), and PA is the Poole-Atkins

coefficient (α/PA=0.01). Of note: When reached the bottom (transparency being greater than water depth), it was replaced with the transparencies synchronously measured from a deeper but homogeneous habitat nearby (Wang et al., 2005b).

By plotting the scatter of total turbidity (1/SD) versus Chl *a* based on our data, the Chl *a* concentration imposes a minimum on the reciprocal of Secchi-disk transparency. This minimum can be described according to Eq3 with:

$$\frac{1}{SDmax} = 0.56 + 0.01\text{Chl } a \ldots\ldots\ldots\ldots\ldots\ldots\ldots\ldots Eq4$$

In Eq4, the Chl *a* concentration imposes a minimum on the total turbidity that is defined as $Turb_{Alg}$. $Turb_{NonAlg}$ can be expressed as Eq5 according to Eq3 and Eq4:

$$Turb_{NonAlg} = \frac{1}{SD} - 0.56 - 0.01\text{Chl } a \ldots\ldots\ldots\ldots Eq5.$$

2.5. Statistical analyses

Non-parametric tests, including Friedman and Wilcoxon-Nemenyi-McDonald-Thompson post-hoc tests, were conducted to detect the differences between treatments for single-sample repeated measures data (Kim, 2014). All the *p*-values can be found in the supplementary material (Table S1). One-way analysis of variance (ANOVA) was used to test the differences in fish growth conditions between the treatments. We used a linear mixed-effect model to explore variation in two response variables (TP and L_{RR}) using the following model:

$$\begin{aligned} y_{i,j} = \alpha &+ \beta_1 \times TN_{i,j} + \beta_2 \times Temp + \beta_3 \times Sed_{typ} \\ &+ \beta_4 \times TN \times Temp + \beta_5 \times TN \times Sed_{typ} \\ &+ \beta_6 \times Temp \times Sed_{typ} \\ &+ a_i \\ &+ b_i \\ &+ \varepsilon_{i,j} \ldots\ldots\ldots\ldots\ldots\ldots\ldots\ldots\ldots\ldots\ldots\ldots Mod\ 1 \end{aligned}$$

where

$$a_i \sim N(0, \sigma_{0i}^2)$$

$$b_i \sim N(0, \sigma_{1i}^2)$$

$$\varepsilon_{i,j} \sim N(0, \sigma^2)$$

Here, $y_{i,j}$ is the mean standardized TP or L_{RR}. $TN_{i,j}$ is a continuous variable representing the concentration of TN. $Temp_{i,j}$ is a continuous variable representing the temperature of water. $Sed_{typ}{}_{i,j}$ is a categorical variable representing the characteristics and trophic level of the sediment (Sed_{Low}: loam with low OM; Sed_{High}: clay with high OM). a_i and b_i are random adjustments to the intercepts and slopes of relationships with year for time series i, allowing the analysis to account for effects specific for each time series. For model 1, we only included three independent variables (TN, Sed_{type}, and seasonal temperature) and their two-way interactions. This was because, on the one hand, inclusion of too many factors is not conducive to model visualization (plots constructed from model output), which is essential to mitigate the risk of over-interpreting the final model coefficients; on the other hand, there were too few observations in some combinations of multiple discrete predictors to allow robust parameter estimation. Moreover, we introduced an auto-regressive model of order 1 to the error structure to account for the likelihood that residuals for consecutive years in each time series are more correlated than residuals separated by longer intervals. For this, we used function *corCAR1* in the R package *nlme* (Sydeman et al., 2021).

To further depict the process of TP changes in response to potentially influential factors and determine their quantitative relationships, piecewise structural equation modeling (piecewise SEM) was conducted (Lefcheck, 2016). Before constructing the piecewise SEM, multicollinearity among environmental variables (including TN, Chl *a*, $Turb_{Alg}$, $Turb_{NonAlg}$, planktivorous fish, benthic fish, OM_{Sed}, and pH_{Sed}) was diagnosed, and high multi-collinearity was found between $Turb_{Alg}$ and Chl *a* (Variance Inflation Factor, VIF > 10). The multi-collinearity diagnosis was valid (VIF < 5) after the removal of $Turb_{Alg}$. We first developed a model at the conceptual level (including causal assumptions) based on prior theoretical knowledge and statistical data analysis. Then, candidate SEM was fully specified after evaluating specification options such as sample size and model complexity. Finally, model evaluation, comparison, and selection were performed.

3. Results

3.1. Variations in P dynamics and its potential influencing factors

During the experimental period (from August 13th, 2011 to May 27th, 2016), NH_4^+ constituted a high proportion of the TN [38% (24% – 56%), mean (min–max)], followed by NO_3^- [10% (4% – 19%)], while NO_2^- contributed <1% (Fig. 2B). NH_4^+ in the Sed_{Low} ponds showed, as expected, a significant treatment gradient, being significantly higher in N_{5a}, N_{10a}, and N_{25a} than in $N_{0.5a}$, while no difference was observed between N_{1a} and $N_{0.5a}$ (Table S1, Fig. 3). Similar patterns of NH_4^+ were found in Sed_{High} ponds.

In the Sed_{Low} ponds, TP was significantly higher in N_{5a} and N_{25a} than in $N_{0.5a}$, N_{1a}, and N_{10a}. In the Sed_{High} ponds, TP in N_{25b} was significantly higher than in $N_{0.5b}$, N_{1b}, N_{5b}, and N_{10b} (Table S1, Fig. 3). Labile-P in the overlying water (0 – 20 mm) increased with the increasing N gradient (Fig. 4), while the pattern was opposite in the sediment (-100 – 0 mm), where labile-P decreased with increasing N input. Synchronized monitored Fe(Π) showed a pattern similar to labile-P (Fig. 4). As for Chl *a*, it was higher in N_{5a}, N_{10a}, and N_{25a} than $N_{0.5a}$ in the Sed_{Low} ponds, and in the Sed_{High} pond it was higher in N_{25b} than in $N_{0.5b}$ (Table S1, Fig. 3). $Turb_{Alg}$ showed the same pattern as Chl *a*. As for $Turb_{NonAlg}$, it was higher in N_{5a}, N_{10a}, and N_{25a} than in $N_{0.5a}$ in the Sed_{Low} ponds, while no difference was observed in the Sed_{High} ponds (Table S1, Fig. 3). pH in the Sed_{Low} ponds was significantly lower in N_{25a} than in $N_{0.5a}$, while no difference was observed among $N_{0.5a}$, N_{1a}, N_{5a}, and N_{10a}; pH in the Sed_{High} ponds showed the same pattern as in the Sed_{Low} ponds (Table S1, Fig. 3). No significant differences among the treatments were observed for DO and Eh (Table S1, Fig. 3).

Algal composition and biomass are presented in Table S3 and Fig. S6. Eighty-nine species belonging to *Cyanophyta*, *Chlorophyta*, *Bacillariophyta*, *Euglenophyta*, *Chrysophyta*, *Dinophyta*, and *Cryptophyta* were recorded (Table S3). Algal biomass increased with N loading. The increase trend varied with season, being highest in summer, followed by autumn, and lowest in winter and spring (Fig. S6).

More specifically, *Dinophyta* (0.95 mg L^{-1}, mean value in biomass), *Cyanophyta* (0.35 mg L^{-1}), and *Euglenophyta* (0.25 mg L^{-1}) dominated in autumn; *Cyanophyta* (0.21 mg L^{-1}), *Chlorophyta* (0.18 mg L^{-1}), and *Dinophyta* (0.16 mg L^{-1}) dominated in winter; spring phytoplankton was dominated by *Chrysophyta* (0.1 mg L^{-1}) and *Chlorophyta* (0.08 mg L^{-1}); and summer phytoplankton was dominated by *Chlorophyta* (1.29 mg L^{-1}), *Euglenophyta* (1.19 mg L^{-1}), *Cyanophyta* (0.75 mg L^{-1}), and *Dinophyta* (0.41 mg L^{-1}) (Fig. S6).

The high-frequency monitoring data including TP, PO_4^{3-}, Chl *a*, DO, pH, and APA in July, 2015 are presented in Fig. S4. TP and Chl *a* increased rapidly after N addition, being significantly higher in N_{25a} than in N_{5a} and $N_{0.5a}$. However, the rise in Chl *a* postdated the onset of TP, with a lag time of several days. In terms of PO_4^{3-}, no significant differences emerged between N_{25a}, N_{5a}, and $N_{0.5a}$, although it tended to be lower in N_{25a} and N_{5a} than in $N_{0.5a}$. DO was significantly lower in N_{25a} and N_{5a} than in $N_{0.5a}$. As for water pH, it was significantly higher in N_{25a} than in N_{5a}, while no significant difference emerged between N_{25a} and $N_{0.5a}$. APA increased significantly after N addition, being significantly higher in N_{25a} than in N_{5a} and $N_{0.5a}$.

As shown in Table 2, the body weight of silver carp in the Sed_{Low} ponds was significantly higher in N_{25a} and N_{10a} than in $N_{0.5a}$, while no difference was found among N_{1b}, N_{5b}, and $N_{0.5b}$. In the Sed_{High} ponds, the body weight of silver carp was significantly higher in N_{25b}, N_{10b}, N_{5b}, and N_{1b} than in $N_{0.5b}$. The same trend was found for bighead carp in both the Sed_{Low} and the Sed_{High} ponds. As for the body weight of bighead carp, it was significantly higher in N_{25a}, N_{5a}, and N_{1a} than in $N_{0.5a}$ in the Sed_{Low} ponds, while no difference was found between N_{10a} and $N_{0.5a}$. In the Sed_{High} ponds, the body weight of bighead carp was significantly higher in N_{25b} than in N_{10b} and $N_{0.5b}$, while no difference appeared among N_{25b}, N_{5b}, and N_{1b}. As for the fish biomass, the biomass of silver carp in the Sed_{Low} ponds was significantly higher in N_{25a}, N_{10a}, and N_{5a} than in $N_{0.5a}$, while a significantly lower value was found for N_{1a} compared with $N_{0.5a}$. In the Sed_{High} ponds, the total biomass of silver carp was significantly higher in N_{25b}, N_{10b}, N_{5b}, and N_{1b} than in $N_{0.5b}$. The total biomass of bighead carp in the Sed_{Low} ponds N_{25a} and N_{10a} was significantly higher than in $N_{0.5a}$,

while a lower value for N_{5a} and no difference for N_{1a} were found compared with $N_{0.5a}$. In the Sed_{High} ponds, all N-treatments had higher fish biomass than $N_{0.5b}$. As for the total biomass of gibel carp, no statistical difference was found among N_{25a}, N_{10a}, and $N_{0.5a}$ in the Sed_{Low} ponds, while significantly lower values were found in N_{5a} and N_{1a} than in $N_{0.5a}$. In the Sed_{High} ponds, the biomass of gibel carp was significantly higher in N_{25b} than in $N_{0.5b}$, while no difference appeared among N_{10b}, N_{5b}, N_{1b}, and $N_{0.5b}$. In terms of the total biomass of the three fish species, it was significantly higher in N_{25a} and N_{10a} than in $N_{0.5a}$ in the Sed_{Low} ponds, while no difference emerged among N_{5a}, N_{2a}, and $N_{0.5a}$. In the Sed_{High} ponds, N_{25b}, N_{10b}, N_{5b}, and N_{2b} had a significantly higher fish biomass than $N_{0.5b}$. In all ponds, bighead carp had the largest contribution [10,733 g (1676 g – 40906 g), mean (min–max)], followed by silver carp [5,066 g (355 g – 22071 g)] and gibel carp [800 g (373 g – 1291 g)]. Extra information on fish body length can be found in Table 2.

3.2. Changes in sediment properties

TN_{Sed} in both the Sed_{Low} and Sed_{High} ponds, probably due to the settlement of external N additions, showed a significant treatment gradient, which was higher in N_{25a} and N_{25b} than in the other ponds, while no difference was observed among the other ponds (Table S1, Fig. 5A). OM_{Sed} tended to increase in both the Sed_{Low} and the Sed_{High} ponds, although no statistical differences were observed (Table S1, Fig. 5B). A decreasing trend in pH_{Sed} was detected over time, especially in the ponds receiving higher N addition (N_{25a} and N_{25b}) (Table S1, Fig. 5C). No differences in Fe_P, Ca_P, and Org_P were recorded between the ponds (Table S1, Fig. 5D – F). Fe_P tended to decrease after N addition, being consistent with the release of Fe(II) from the sediment determined by diffusive gradients in thin-films. In contrast, Ca_P generally showed an increasing trend. Org-P remained relatively constant during N addition.

3.3. Potential drivers of sediment P release

TP and L_{RR} (log of the response ratio) were used as indicators of N-stimulated sediment P release, with TN, sediment type, seasonal variation of temperature, and

their two-way interactions being considered in the linear mixed models. Both TP and L_{RR} showed an increasing trend with TN (Fig. 6, Table S2). The trends varied with season (water temperature) and were highest in summer, followed by spring and autumn, and lowest in winter. Within each season, TP and L_{RR} varied with sediment type, being higher in the Sed_{High} than in Sed_{Low} ponds.

The Fisher'C and p values in Piecewise SEM were 23.2 and 0.73 (p value > 0.05), indicating that all significant paths were included and that the result of the model was acceptable (Fig. 7). The path coefficients from TN to pH_{Sed} and then to TP were negative and significant. By increasing $Fish_{Pla}$ and $Turb_{NonAlg}$, TN indirectly positively affected the TP increase. The path coefficients from OM_{Sed} to TP and from $Turb_{NonAlg}$ to Chl *a* were positive and significant. It is noteworthy that the cause-effect path relationship between Chl *a* and TP was significant and bidirectional. Overall, TN, pH_{Sed}, Chl *a*, $Turb_{NonAlg}$, $Fish_{Pla}$, and OM_{Sed}, the potential factors regulating the sediment P release, accounted for 92% of the variations in TP.

4. Discussion

4.1. Long-term large-scale effects of N loading on sediment P release

Our 6-year whole-ecosystem experiment revealed no significant P release when TN < 10 mg L^{-1}, while P release was promoted when TN > 25 mg L^{-1}. These results generally agreed with previous mesocosm observations revealing that TN above a certain value (10 mg L^{-1}) can stimulate the sediment P release (Ma et al., 2018). Also, a positive relation between N and P has been observed in natural lakes with NH_4^+ concentrations < 0.5 mg L^{-1} (e.g., Lake Yangdong, Lake Liangzi, etc.) (Li et al., 2016). Interestingly, the TN threshold for promoting, in our case, the P release (with less OM_{Sed}, 1.5 – 33.6 g kg^{-1}) was higher than in a previous mesocosm study (rich in OM_{Sed}, 64 g kg^{-1}) (Ma et al., 2018). In general, the richer the OM content of the sediment, the more pronounced the release of P (Li et al., 2016) because the mineralization of OM can consume a great deal of O_2, which may further result in low redox-related P release. Indeed, the effect of NH_4^+ on P release depended on N loading and sediment OM, i.e., TP and L_{RR} were higher at high N loads and at a high content

of OM in the sediment. The important role played by the sediment OM content in P dynamics is increasingly recognized (Li et al., 2016; Deng et al., 2022). For example, OM accumulation in most forms (such as glucose, acetate, formate, and macrophyte material) has been found to stimulate the sediment P release (Watts, 2000; Mitchell et al., 2005; Ahlgren et al., 2011). Consistent with most previous studies, the piecewise SEM determined in our study confirmed a direct positive contribution of OM_{Sed} to the TP increase, probably through enzymatic hydrolysis (APA increased from 305 to 489 μg P g^{-1} h^{-1} in N_{25a}, Fig. S4) and anaerobic desorption (DO in N_{25a} decreased to below 3 mg L^{-1}, Fig. S4).

We further found that the TP increase varied over the season, being most apparent in summer, followed by spring and autumn, whereas it was almost unnoticeable in winter. This pattern may be attributed to temperature-regulated sediment mineralization rates, which are higher at warmer than at colder temperatures (Jensen & Andersen, 1992; Søndergaard et al, 2003; Anthony & Lewis, 2012), and to an overall higher algal production in summer, which, in turn, leads to mineralization of newly settled OM and oxygen consumption in the sediment, and thus P release.

4.2. Critical mechanisms of N-driven P release in large-scale experiments

We developed a conceptual diagram to elucidate potential mechanisms behind the effect of NH_4^+ on sediment P release under conditions closer to those of natural lakes (Fig. 8). The N-promoted sediment P release at ecosystem scale observed in our study partially agrees with previous short-term and small-scale observations revealing that high NH_4^+ addition can stimulate P release by increasing APA, followed by increase in phytoplankton production, and reduced DO when decomposition of some of these phytoplankton occur at the sediment surface (Ma et al., 2018). At larger experimental scale, however, more factors (e.g., bioturbation) may also be involved (Wang et al., 2022; Mao et al., 2020; Tammeorg et al., 2016). Specifically, the mechanisms underlying the effects of NH_4^+ on sediment P release could be fourfold at ecosystem scale. Firstly, to counteract the stoichiometric N:P imbalance caused by excessive NH_4^+ input, phytoplankton may promote the release of sediment P through a

"pumping" effect and alkaline phosphatase production (Xie et al., 2003; Ma et al., 2018). We found that phytoplankton, when abundant, almost depleted PO_4^{3-} in the water (PO_4^{3-} in N_{25a} dropped below 0.01 mg L^{-1}), creating a steeper gradient of PO_4^{3-} concentration at the sediment-water interface that potentially favors the upward diffusion of sediment P (referred to as "pumping" effect in a previous study by Xie et al., 2003). Secondly, N-induced sediment acidification (pH_{Sed} decreased from 7.7 to 6.2 in the higher N treatment) may increase the sediment P release (standardized effect size = 56%), partly due to the dissolution of detrital apatite (Cooke et al., 2005). This mechanism has also been shown to be of importance in many long-term terrestrial N addition experiments (Hao et al., 2020; Wang et al., 2022). For example, in a 10-year field test, N enrichment promoted the dissolution of immobile P (mainly Ca-bound recalcitrant P) to more available forms of P by decreasing soil pH from 7.6 to 4.7, likely due to the H^+ production induced by N transformations (Wang et al., 2022).

Thirdly, the increase of TP caused by sediment release may further fuel sediment P release by forming a "TP-phytoplankton-fish" positive feedback loop (Fig. 7). In this loop, increased TP stimulates the growth of phytoplankton, which in turn increases the biomass of pelagic fish (Table 2), reflecting that the increase of phytoplankton biomass increases the food availability for the fish (directly or indirectly). With a higher biomass of cyprinids, sediment disturbance increases, leading to more P in the water and subsequently more phytoplankton and more fish (Fig. 7). The important role of pelagic fish in the P transport from sediment to the water column via disturbance has been widely recognized (Persson, 1997; Huser et al., 2016; Mao et al., 2020); such sediment disruption may also result in much steeper concentration gradients favoring P release through diffusion (Tammeorg et al., 2016; 2020). Contrary to $Fish_{Pla}$, $Fish_{Ben}$ (accounting for only 8% of the total fish biomass) seemed to be unaffected by the N input (likely due to its non-algal feeding habit) and did apparently not contribute to sediment resuspension either, as suggested by the non-significant path coefficients from TN to $Fish_{Ben}$ and from $Fish_{Ben}$ to $Turb_{NonAlg}$ in the piecewise SEM (Fig. 7). This difference may be attributed to differences in their

diet: both silver carp and bighead carp are planktivores, and their growth rates naturally depend on the amounts of plankton available (Cremer & Smitherman, 1980), while gibel carp are omnivores and their growth does therefore not rely significantly on the amount of phytoplankton (Xie et al., 2001). A similar pattern as traced in our study was found by Wang et al. (2017), showing that the body weights of silver carp (R^2 = 0.55, p = 0.01) and bighead carp (R^2=0.55, p=0.01) were highly positively correlated with Chl *a*, while that of gibel carp was only weakly related to Chl *a*.

Finally, consistent with the anoxic-desorption release of P reported in most previous studies (Nürnberg, 1995; Ma et al., 2018), the formation of anoxic or low redox conditions at the sediment-water interface (DO < 3 mg L^{-1}, as indicated by the high-frequency monitoring data in Fig. S4) did indeed cause the reductive dissolution of Fe(III) oxyhydroxides and release of Fe_P, as suggested by the synchronous release of Fe(Π) and labile-P as well as the reduction of Fe_P in sediment. Besides, NH_4^+ nitrification and decomposition of OM in the sediment may lead to low redox conditions in the surface sediment (Li et al., 2016). Notably, the anoxic-desorption release in our case was partially masked by the water mixing (i.e., water O_2 replenishment) likely caused by fish disturbance or wind activity (e.g., long-term monitored DO levels remained ca. 8 mg L^{-1}, Fig. 3) as the released Fe(Π) may recombine with PO_4^{3-} in the water (Carignan & Flett, 1981; Gomez et al., 1998).

4.3. Insights on a step forward from the mesocosm to the large-scale test

Short-term mesocosm tests are the most frequently used approach to elucidate sediment P behavior as they allow highly replicable, controlled experimental conditions and simplification of tested factors (Schindler, 1998; Jiang et al., 2008; Ma et al., 2018; 2021). Although mesocosm tests have led to similar conclusions as our large-scale study, the involved processes and mechanisms differ, likely because the mesocosms typically lack the complexity of lakes, in particular natural mixing regimes and whole organism communities. Stronger mixing of natural lakes could weaken the anoxic-desorption release of P by increasing the replenishment of water O_2, and wide-ranging organisms would enhance the contribution of bioturbation to the sediment P release compared with P diffusion. Moreover, mesocosm experiments are

typically too short (less than one season) to accurately assess the response of slow-responding biogeochemical processes such as sediment acidification as a consequence of long-term N application (favoring P release) (Wang et al., 2022). Thus, besides large-scale experiments, future mesocosm experiments in should also mimic the natural hydrodynamics and community compositions and be run for a longer time to properly extrapolate the results to natural lakes.

5. Conclusions

In our experiment, the following results were obtained:

(i) NH_4^+ loading promoted the P release from the sediment. The magnitude of the promotion largely depended on the amount of NH_4^+ loading and was relatively pronounced when TN >10 – 25 mgL^{-1}.

(ii) The N-stimulated P increase varied with season and sediment type, showing more pronounced increases in TP in summer and in sediments with high OM than in winter and in sediments with low OM.

(iii) According to the piecewise structural equation modeling, N-induced phytoplankton pumping, acidification, and fish disturbance were important mechanisms underlying the N-stimulated sediment P release. In addition, OM_{Sed} positively contributed to the sediment P release, demonstrating the highest P release in OM-rich sediments.

(iv) Compared with mesocosm tests, N-driven sediment P release at ecosystem scale involved novel mechanisms such as sediment acidification and resuspension caused by bioturbation (due to higher fish biomass). Our case study is an essential step in extrapolating the N and P co-relationship and in understanding and managing lake eutrophication.

Acknowledgements

The research was sponsored by National Natural Science Foundation of China (42107399), Zhejiang Basic Public Welfare Research Program (LQ21C030005), Ningbo Public Welfare Science and Technology Program (2021S060), National Key Research and Development Program of China (2021YFC3200103), Yunnan

Provincial Department of Science and Technology (202001BB050078; 202103AC100001), and Key Research and Development Program of Hubei Province (2022BCA072). Haijun Wang was supported by the Youth Innovation Association of Chinese Academy of Sciences as an excellent member (Y201859). EJ was supported by the TÜBITAK program BIDEB2232 (project 118C250) and ANAEE-Denmark. MS was supported by Poul Due Jensen Foundation. We thank Anne Mette Poulsen for valuable English editions.

References

Abad-Valle, P., Alvarez-Ayuso, E., Murciego, A., 2015. Evaluation of ferrihydrite as amendment to restore an arsenic-polluted mine soil. Environ. Sci. Pollut. Res. 22 (9), 6778–6788. Doi: 10.1007/s11356-014-3868-6.

Ahlgren, J., Reitzel, K., De Brabandere, H., Gogoll, A., Rydin, E., 2011. Release of organic P forms from lake sediments. Water Res. 45, 565–572. Doi: 10.1016/j.watres.2010.09.020.

Anthony, J.L., Lewis, W.M., 2012. Low boundary layer response and temperature dependence of nitrogen and phosphorus releases from oxic sediments of an oligotrophic lake. Aquat. Sci. 74 (3), 611–617. Doi: 10.1007/s00027-012-0255-6.

Carignan, R., Flett, R.J., 1981. Postdepostional mobility of phosphorus in lake sediment. Limnol. Oceanogr. 26, 363–366.

Cooke, G.D., Welch, E.B., Peterson, S.A., Nichols, S.A., 2005. Restoration and management of lakes and reservoirs. CPC Press, Taylor & Francis Group 6000 Broken Sound Parkway NW, Suite 300. Boca Raton, pp. 208–220.

Cremer, M.C., Smitherman, R.O., 1980. Food habits and growth of silver and bighead carp in cages and ponds. Aquaculture 20, 57–64.

Deng, P.Y., Yi, Q.T., Zhang, J., Wang, C.H., Chen, Y.H., Zhang, T., et al., 2022. Phosphorous partitioning in sediments by particle size distribution in shallow lakes: from its mechanisms and patterns to its ecological implications. Sci. Total Environ. 814, (152753). Doi: 10.1016/j.scitotenv.2021.152753.

Golterman, H.L., 1996. Fractionation of sediment phosphate with chelating

compounds: a simplification, and comparison with other methods. Hydrobiologia 335 (1), 87–95. Doi: 10.1007/bf00013687.

Gomez, E., Fillit, M., Ximenes, M.C., Picot, B. 1998. Phosphate mobility at the sediment-water interface of a Mediterranean lagoon (Etang du Mejean), seasonal phosphate variation. Hydrobiologia 374, 203–216.

Gruber, N., Galloway, J.N., 2008. An earth-system perspective of the global nitrogen cycle. Nature 451(7176), 293–296. Doi: 10.1038/nature06592

Hao, T.X., Zhu, Q.C., Zeng, M.F., Shen, J.B., Shi, X.J., Liu, X.J., et al., 2020. Impacts of nitrogen fertilizer type and application rate on soil acidification rate under a wheat-maize double cropping system. J. Environ. Manage. 270, 110888. Doi: 10.1016/j.jenvman.2020.110888.

Huser, B.J., Bajer, P.G., Chizinski, C.J., Sorensen, P.W., 2016. Effects of common carp (*Cyprinus carpio*) on sediment mixing depth and mobile phosphorus mass in the active sediment layer of a shallow lake. Hydrobiologia 763 (1), 23–33. Doi: 10.1007/s10750-015-2356-4.

Jensen, H.S., Andersen, O.F., 1992. Importance of temperature, nitrate and pH for the phosphate release from aerobic sediments of four shallow eutrophic lakes. Limnol. Oceanogr. 37(3), 577589.

Jeppesen, E., Søndergaard, M., Jensen, J.P., Havens, K.E., Anneville, O., Carvalho, L., et al., 2005. Lake responses to reduced nutrient loading-an analysis of contemporary long-term data from 35 case studies. Freshw. Biol. 50, 1747–1771. Doi: 10.1111/j.1365-2427.2005.01415.x.

Jiang, X., Jin, X., Yao, Y., Li, L., Wu, F., 2008. Effects of biological activity, light, temperature and oxygen on phosphorus release processes at the sediment and water interface of Taihu Lake, China. Water Res. 42 (8–9), 2251–2259. Doi: 10.1016/j.watres.2007.12.003.

Kim, H.Y., 2014. Statistical notes for clinical researchers: Nonparametric statistical methods: 2. nonparametric methods for comparing three or more groups and repeated measures. Restorative dentistry & endodontics 39 (4), 329–332. Doi: 10.5395/rde.2014.39.4.329.

Lefcheck, J.S., 2016. PiecewiseSEM: piecewise structural equation modelling in R for ecology, evolution, and systematics. Methods Ecol. Evol. 7, 573–579. Doi: 10.1111/2041-210X.12512.

Li, H., Song, C.L., Cao, X.Y., Zhou, Y.Y., 2016. The phosphorus release pathways and their mechanisms driven by organic carbon and nitrogen in sediments of eutrophic shallow lakes. Sci. Total Environ. 572, 280–288. Doi: 10.1016/j.scitotenv.2016.07.221.

Liu, Y.B., Guo, Y.X., Song, C.L., Xiao, W.J., Huang, D.Z., Cao, X.Y., et al., 2009. The effect of organic matter accumulation on phosphorus release in sediment of Chinese shallow lakes. Fund. Appl. Limnol. 175 (2), 143–150.

Liu, M.X., Huang, X., Song, Y., Tang, J., Cao, J., Zhang, X.Y., et al., 2019. Ammonia emission control in China would mitigate haze pollution and nitrogen deposition, but worsen acid rain. Pnas 116, 7760–7765. Doi: 10.1073/pnas.1814880116.

Marklein, A.R., Houlton, B.Z., 2012. Nitrogen inputs accelerate phosphorus cycling rates across a wide variety of terrestrial ecosystems. New phytol. 193 (3), 696–704. Doi: 10.1111/j.1469-8137.2011.03967.x.

Ma, S.N., Wang, H.J., Wang, H.Z., Li, Y., Liu, M., Liang, X.M., et al., 2018. High ammonium loading can increase alkaline phosphatase activity and promote sediment phosphorus release: a two-month mesocosm experiment. Water Res. 145, 388–397. Doi: 10.1016/j.watres.2018.08.043.

Ma, S.N., Wang, H.J., Wang, H.Z., Zhang, M., Li, Y., Shi, J.B., et al., 2021. Effects of nitrate on phosphorus release from lake sediments. Water Res. 194 (2021), 116894.

Mao, Z.G., Gu, X.H., Cao, Y., Zhang, M., Zeng, Q.F., Chen, H.H., et al., 2020. The role of top-down and bottom-up control for phytoplankton in a subtropical shallow eutrophic lake: evidence based on long-term monitoring and modeling. Ecosystems 23, 1449–1463. Doi: 10.1007/s10021-020-00480-0.

Meijer, M.L., Jeppesen, E., van Donk, E., Moss, B., Scheffer, M., Lammens, E., et al., 1994. Long-term responses to fish-stock reduction in small shallow lakes: interpretation of five-year results of four biomanipulation cases in the

Netherlands and Denmark. Hydrobiologia 275 (276), 457–466.

Mitchell, A.M, Baldwin, D.S., Rees, G.N., 2005. Alterations to potential phosphorus release processes from anaerobic freshwater sediments with additions of different species of labile carbon. In: Serrano L, Golterman H (eds) Phosphates in sediments, Backhuys Publishers, Kerkwerve, The Netherlands, pp. 43–45.

Nürnberg, C.K., 1995. Quantifying anoxia in lakes. Limnol. Oceanogr. 40 (6), 1100–1111.

Portielje, R., Van der Molen, D.T., 1999. Relationships between eutrophication variables: from nutrient loading to transparency. Hydrobiologia 408, 375–387.

Li, Y., Wang, H.Z., Liang, X.M., Yu, Q., Xiao, X.C., Shao, J.C., et al., 2017. Total phytoplankton abundance is determined by phosphorus input: evidence from an 18-month fertilization experiment in four subtropical ponds. Can. J. Fish. Aquat. Sci. 74 (9), 1454–1461. Doi: 10.1139/cjfas-2016-0057.

Peñuelas, J., Sardans, J., 2022. The global nitrogen-phosphorus imbalance. Science 375 (6578), 266–267. Doi: 10.1126/science.abl4827.

Peñuelas, J., Janssens, I.A., Ciais, P., Obersteiner, M., Sardans, J., 2020. Anthropogenic global shifts in biospheric N and P concentrations and ratios and their impacts on biodiversity, ecosystem productivity, food security, and human health. Glob. Change Biol. 26 (4), 1962–1985. Doi: 10.1111/gcb.14981.

Persson, A., 1997. Phosphorus release by fish in relation to external and internal load in a eutrophic lake. Limnol. Oceanogr. 42 (3), 577–583. Doi: 10.4319/lo.1997.42.3.0577.

Pettersson, K., Istvanovics, V., 1988. Sediment phosphorus in Lake Balaton-Forms and mobility. Arch Hydrobiol Beilh Ergenbn Limnol. 30, 25–41.

Psenner, R., Pucsko, R., Sager. M., 1984. Die Fraktionierung organischer und anorganischer Phosphorverbindungen von Sedimenten-Versuch einer Definition kologisch wichtiger Fraktionen. Arch. Hydrobiol. 70, 111–115.

Ripl, W., 1976. Biochemical oxidation of polluted lake sediment with nitrate: A new lake restoration method. Ambio 5 (3), 132–135.

Schindler, D.W., 1998. Replication versus realism: The need for ecosystem-scale

experiments. Ecosystems 1 (4), 323–334. Doi:10.1007/s100219900026.

Søndergaard, M., Jeppesen, E., Jensen, J.P., 2000. Hypolimnetic nitrate treatment to reduce internal phosphorus loading in a stratified lake. Lake Reservoir Manag. 16 (3), 195–204. Doi: 10.1080/07438140009353963.

Søndergaard, M., Jensen, J.P., Jeppesen, E., 2003. Role of sediment and internal loading of phosphorus in shallow lakes. Hydrobiologia 506–509 (1–3), 135–145. Doi: 10.1023/b:hydr.0 0 0 0 0 08611.12704.dd.

Sydeman, W.J., Schoeman, D.S., Thompson, S.A., 2021. Hemispheric asymmetry in ocean change and the productivity of ecosystem sentinels. Science 372 (6545), 980–983.

Tarvainen, M., Ventela, A.M., Helminen, H., Sarvala, J., 2005. Nutrient release and resuspension generated by ruffe (*Gymnocephalus cernuus*) and chironomids. Freshwat. Biol. 50, 447–458.

Tammeorg, O., Horppila, J., Tammeorg, P., Haldna, M., Niemisto, J., 2016. Internal phosphorus loading across a cascade of three eutrophic basins: A synthesis of short- and long-term studies. Sci. Total Environ. 572, 943–954. Doi: 10.1016/j.scitotenv.2016.07.224.

Tammeorg, O., Nurnberg, G., Horppila, J., Haldna, M., Niemistö, J., 2020. Redox-related release of phosphorus from sediments in large and shallow Lake Peipsi: evidence from sediment studies and long-term water monitoring data. J. Great Lakes Res. 46(6), 1595–1603. Doi: 10.1016/j.jglr.2020.08.023.

Wang, R., Yang, J., Liu, H., Sardans, J., Zhang, Y., Wang, X., et al., 2022. Nitrogen enrichment buffers phosphorus limitation by mobilizing mineral-bound soil phosphorus in grasslands. Ecology. 103 (3), e3616. Doi: 10.1002/ecy.3616 e3616.

Wang, S.R., Jin, X.C., Pang, Y., Zhao, H.C., Zhou, X.N., Wu, F.C., 2005a. Phosphorus fractions and phosphate sorption characteristics in relation to the sediment compositions of shallow lakes in the middle and lower reaches of the Yangtze River region, China. J. Colloid Interf. Sci. 289, 339–346.

Wang, H.Z., Wang, H.J., Liang, X.M., Ni, L.Y., Liu, X.Q., Cui, Y.D., 2005b.

Empirical modelling of submersed macrophytes in Yangtze lakes. Ecol. Model. 188, 483–491.

Wang, H.J., Xiao, X.C., Wang, H.Z., Li, Y., Yu, Q., Liang, X.M., et al., 2017. Effects of high ammonia concentrations on three cyprinid fish: Acute and whole-ecosystem chronic tests. Sci. Total Environ. 598, 900–909. Doi: DOI10.1016/j.scitotenv.2017.04.070.

Watts, C.J., 2000. The effect of organic matter on sedimentary phosphorus release in an Australian reservoir. Hydrobiologia 431, 13–25. Doi: 10.1023/A:1004046103679.

Wu, Z., Li, J.C., Sun, Y.X., Penuelas, J., Huang, J.L., Sardans, J., et al., 2022. Imbalance of global nutrient cycles exacerbated by the greater retention of phosphorus over nitrogen in lakes. Nat. Geosci. 15, 464–468. Doi: 10.1038/s41561-022-00958-7.

Xie, L.Q., Xie, P., Li, S.X., Tang, H.J., Liu, H., 2003. The low TN: TP ratio, a cause or a result of microcystis blooms? Water Res. 37 (9), 2073–2080. Doi: 10.1016/S0043-1354(02)00532-8.

Xie, S., Zhu, X., Cui, Y., Wootton, R.J., Lei, W., Yang, Y.X., 2001. Compensatory growth in the gibel carp following feed deprivation: temporal patterns in growth, nutrient deposition, feed intake and body composition. J. Fish Biol. 58, 999–1009.

Yu, C.Q., Huang, X., Chen, H., Charles, H., Godfray, H.C.J., Wright, J.S., et al., 2019. Managing nitrogen to restore water quality in China. Nature 567 (7749), 516–520.

Zeng, M.F., de Vries, W., Bonten, L.T.C., Zhu, Q.C., Hao, T.X., Liu, X.J., et al., 2017. Model-based analysis of the long-term effects of fertilization management on cropland soil acidification. Environ. Sci. Technol. 51 (7), 3843–3851. Doi: 10.1021/acs.est.6b05491.

Graphical Abstract

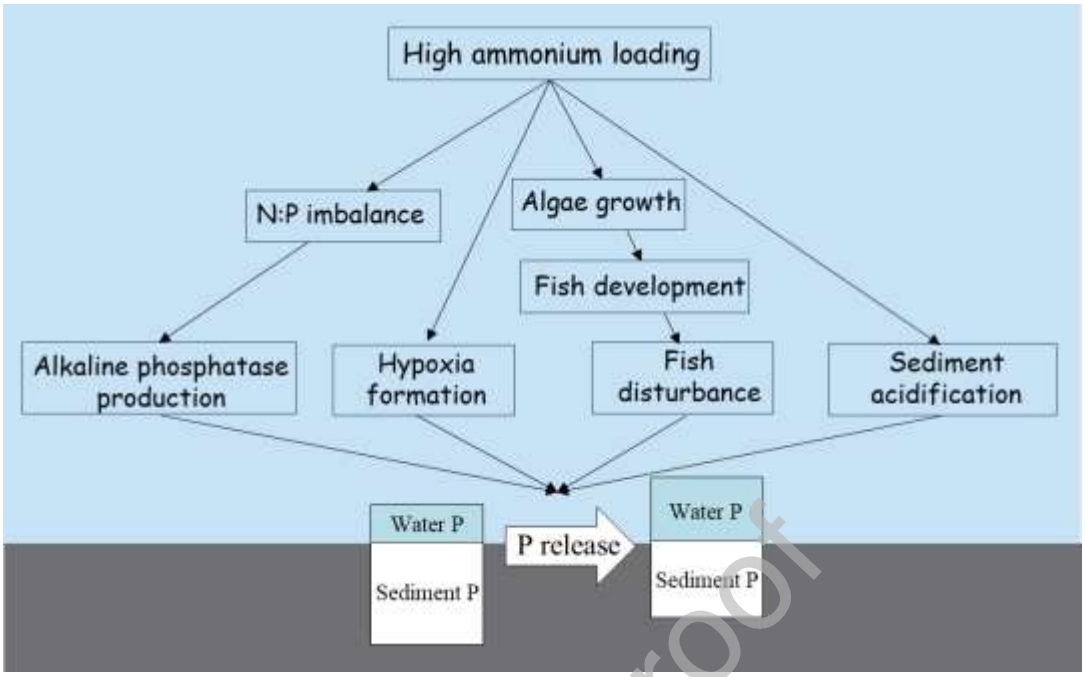

Table 1. Physical and chemical characteristics of the sediment in the ten experimental ponds.

Sed_{Typ}	Sed_{Low}					Sed_{High}				
Pond	$N_{0.5a}$	N_{1a}	N_{5a}	N_{10a}	N_{25a}	$N_{0.5b}$	N_{1b}	N_{5b}	N_{10b}	N_{25b}
OM_{Sed}	9.4	1.5	6.8	4.7	8.4	26.6	17.3	26.0	24.0	33.6
TN_{Sed}	0.8	0.7	1.0	1.0	1.2	1.4	1.3	1.6	1.7	1.9

TP_{Sed}	0.4	0.4	0.3	0.5	0.3	0.4	0.4	0.4	0.4	0.4
Clay	22	25	18	22	24	43	44	41	43	36
Silt	56	59	52	62	57	33	31	35	34	43
Sand	22	16	20	16	19	24	25	24	23	21
pH_{Sed}	7.6	7.8	7.7	7.6	7.6	7.8	7.8	7.7	7.7	7.7

Note: OM_{Sed}, organic matter (g kg^{-1} dw); TN_{Sed}, total nitrogen (g kg^{-1} dw); TP_{Sed}, total phosphorus (g kg^{-1} dw). Silt, sediment silt content (%); Clay, sediment clay content (%); Sand, sediment sand content (%). The value after N indicates the target concentration of total nitrogen, a and b represent low organic matter ponds (coded as Sed_{Low}) and high organic matter ponds (Sed_{High}) of the same nitrogen treatment.

Table 2. Body length (BL, mean±SE), body weight (BW, mean±SE), biomass (kg), and total biomass (TBM) of the three cyprinid fish captured in the middle of the experiment (November, 2013).

Sediment type		Planktivorous fish						Benthic fish		Total fish	
		Sliver carp			Bighead carp			Gibel carp		Sum	
	Pond	BL (cm)	BW (g)	Biomass (kg)	BL (cm)	BW (g)	Biomass (kg)	BL (cm)	BW (g)	Biomass (g)	TBM (g)
Sed_{Low}	$N_{0.5}$	18.2±0.8 d	56.2±10.8 c	1.12 e	27.6±1.4 c	268.9±37.0 c	5.38 d	13.6±0.4 b	44.1±4.2 b	0.84 a	7340 c
	N_1	12.1±0.7 c	17.8±3.0 c	0.36 d	31.2±0.3 b	303.2±1.04 c	4.85 d	19.7±1.7 a	124.5±32 a	0.37 bc	5580 c
	N_5	19.7±0.6 bd	81.4±7.9 bc	1.63 c	30.3±0.4 bc	279.3±7.9 c	1.68 c	18.4±0.4 a	97.8±5.2 a	0.49 b	3794 c
	N_{10}	21.2±1.4 b	160.1±10.1 b	2.4 b	42.7±1.9 a	959.7±99.2 b	10.56 b	11.8±0.9 b	32.6±10.0 b	0.65 ab	13611 b
	N_{25}	43.4±1.4 a	950.4±26.8 a	11.4 a	45.8±0.5 a	1114.2±37.9 a	16.71 a	17.3±1.8 a	97.2±27.8 a	0.87 a	28992 a
Sed_{High}	$N_{0.5}$	14.4±0.4 d	26.8±1.4 e	0.54 e	26.8±3.7 d	229.6±136.3 d	2.1 d	17.4±0.5 a	93.3±5.0 bc	0.75 c	3379 d
	N_1	30.2±0.8 c	292.4±21.0 bd	5.85 d	33.7±0.8 c	471±31.3 cd	9.42 c	20.4±0.5 a	143.7±14.1 ac	0.86 c	16133 bc
	N_5	23.6±0.5 b	154.8±9.7 c	1.86 c	34.3±0.6 c	509.9±23.1 c	10.2 c	19.4±0.6 a	126.1±12.2 ac	1.14 bc	13190 c
	N_{10}	25.2±0.8 b	201.3±18.2 bc	3.42 b	41.0±1.4 b	790.3±47.5 b	5.53 b	18.1±0.7 a	92.5±10.0 bc	0.74 c	9694 b
	N_{25}	47.7±1.0 a	1104.4±72.8 a	22.08 a	60.4±0.6 a	2556.63±92.6 a	40.91 a	19.5±3.2 a	184.4±68.9 a	1.29 ab	64276 a

Note: $N_{0.5}$–N_{25} in the pond column refers to different target concentrations of total nitrogen; Sed_{Low} and Sed_{High} represent low organic matter ponds and high organic matter ponds. Different letters in the same columns of each denote a significant difference at $p < 0.05$ between treatments (one-way ANOVA statistics). The highest value in each column is labeled "a".

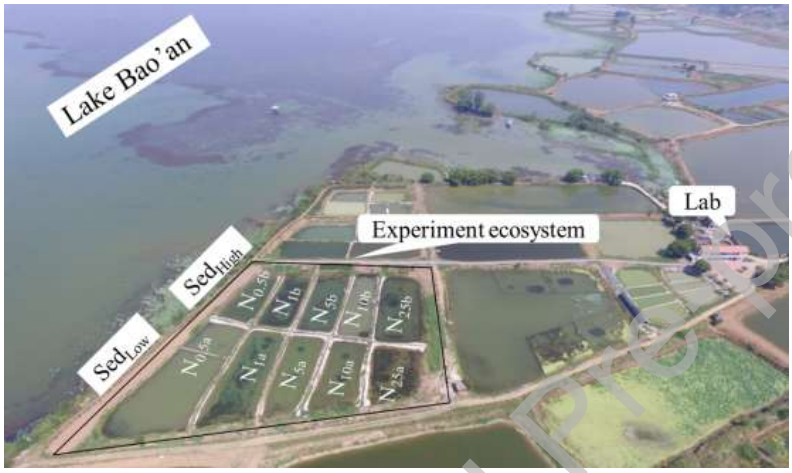

Fig. 1. The pond experimental system. The ponds were grouped into low organic matter ponds (coded as Sed_{Low}) and high organic matter ponds (Sed_{High}). The value after N indicates the target concentration of total nitrogen, a and b represent Sed_{Low} and Sed_{High} ponds of the same nitrogen treatment.

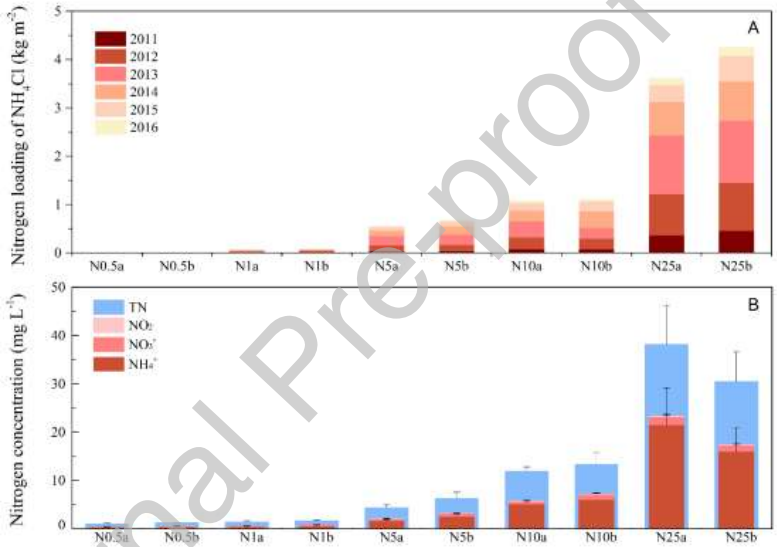

Fig. 2. Loading of NH_4Cl (A) and mean concentrations of different nitrogen forms (B) for various treatments during the experiments (from August 13, 2011 through May 27, 2016). The value after N indicates the target concentration of total nitrogen, a and b represent low organic matter ponds (coded as Sed_{Low}) and high organic matter ponds (Sed_{High}) of the same nitrogen treatment.

Fig. 3. Dynamics in the concentrations of nutrients and important environmental variables associated with nitrogen and phosphorus cycling for various treatments during the experiments (from 2011 through 2016). Sed_{Low}: loam with low organic matter (turquoise); Sed_{High}: clay with high organic matter (purple). TN, total nitrogen concentration (mg L^{-1}); NH_4^+, ammonium concentration (mg L^{-1}); NO_3^-, nitrate concentration (mg L^{-1}); TP, total phosphorus concentration (mg L^{-1}); Chl *a*, phytoplankton chlorophyll *a* (µg L^{-1}); $Turb_{Alg}$, algal turbidity (m^{-1}); $Turb_{NonAlg}$, non-algal turbidity (m^{-1}). DO, dissolved oxygen (mg L^{-1}); Eh, redox potential (mV). The value after N indicates the target concentration of total nitrogen.

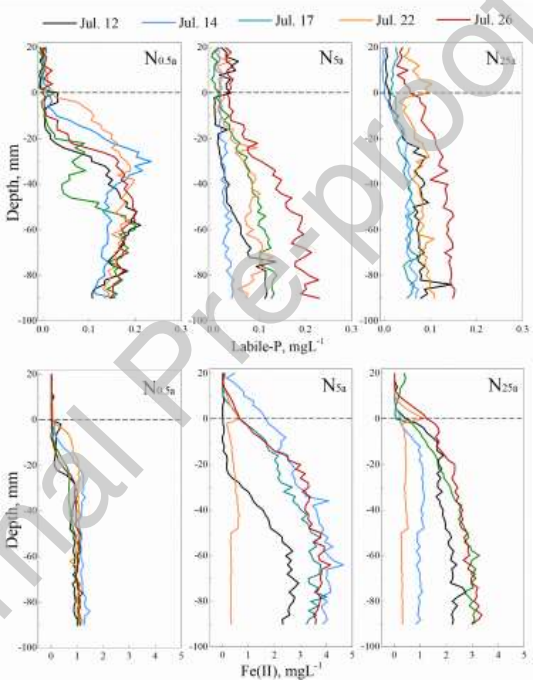

Fig. 4. The distribution of labile phosphorus (labile-P) and Fe(II) in overlying water (0 – 20 mm) and sediment (-100 – -20 mm) profiles on July

12th, 14th, 17th, 22nd, and 26th, 2015 (fertilization was conducted on July 12). The location of the sediment-water interface (dashed line) is represented by zero. $N_{0.5a}$, N_{5a}, and N_{25a} indicate low organic matter ponds with the target nitrogen concentration of 0.5, 5, and 25 mg N L^{-1}.

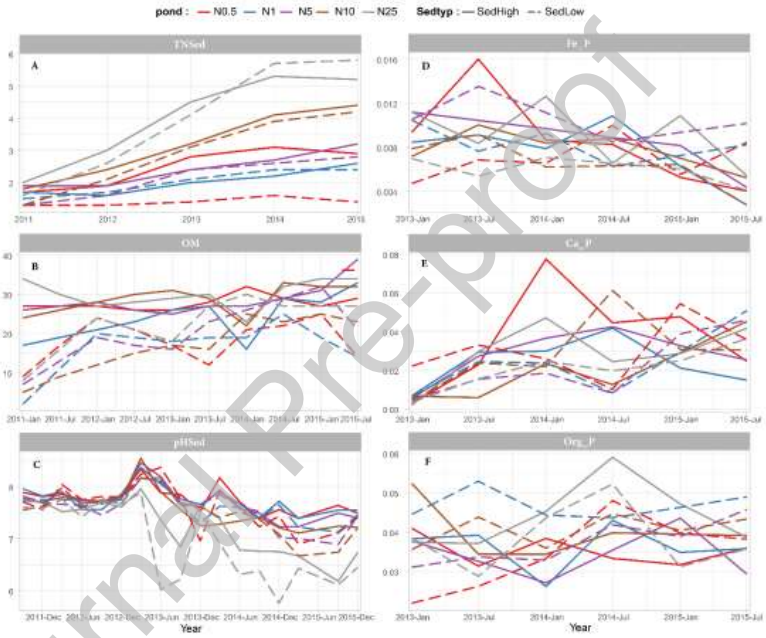

Fig. 5. Temporal variation in surface 5 cm sediment properties. A. TN_{Sed}, total nitrogen content in sediment (g kg^{-1} dw); B. OM, organic matter in sediment (g kg^{-1} dw); C. pH_{Sed}, sediment pH; D. Fe_P, iron-bound phosphorus (mg g^{-1} dw); E. Ca_P, calcium-bound phosphorus (mg g^{-1} dw); F. Org_P, organic phosphorus (mg g^{-1} dw).

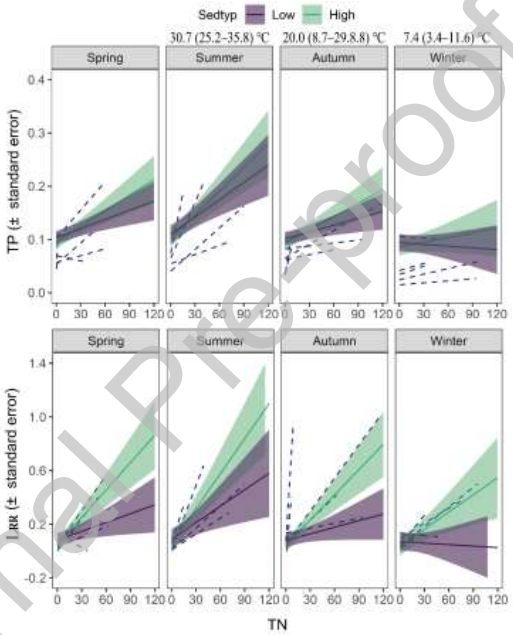

Fig. 6. Modeled trends of total phosphorus concentration (TP, mg L^{-1}) and Log response ratio of TP (L_{RR}). TP (A) and L_{RR} (B) by sediment type (Sed_{Low}: loam with low organic matter, purple; Sed_{High}: clay with high organic matter, turquoise) and season as a function of total nitrogen concentration (TN, mg L^{-1}). Variance explained by fixed and random effects (R^2 = 0.4 and 0.2 for TP and L_{RR}). Trends in individual time series (random effect, dashed lines) are shown as background. The values above the graph indicate the water temperature in the corresponding season

[Mean (Min–Max)]. See the supplementary materials and methods for model details. See Supplementary Table S2 and Fig. S5 for model selection.

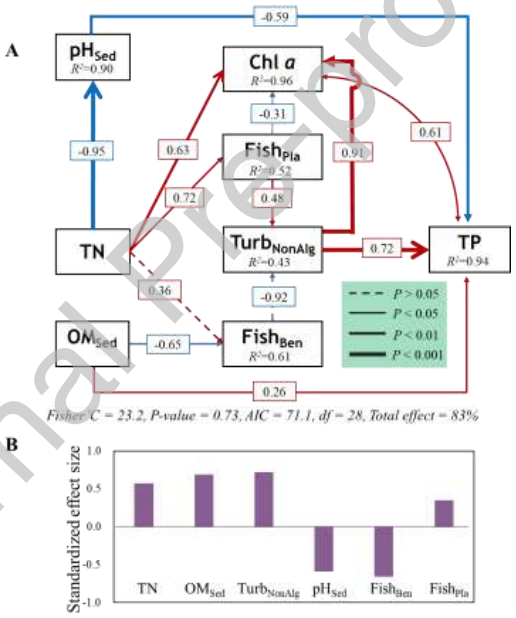

Fig. 7. Piecewise structural equation modeling (Piecewise SEM) for the drivers of total phosphorus concentrations in ponds (A). In the SEM, boxes represent measured variables. Single-headed arrows represent unidirectional relationships among variables. The two-way arrow represents the correlation between the variables. Dotted arrows are insignificant at $p < 0.05$ but retained in the model based on model selection criteria. Blue and red arrows denote negative and positive relationships, respectively. The thickness of the significant paths is scaled based on the magnitude of the standardized regression coefficient. The proportion of the variance explained by predictors (R^2) appears alongside each response variable in the model. (B) The standardized total effect size of every variable on the total phosphorus concentration was calculated as the sum of the significant direct and indirect path coefficients.

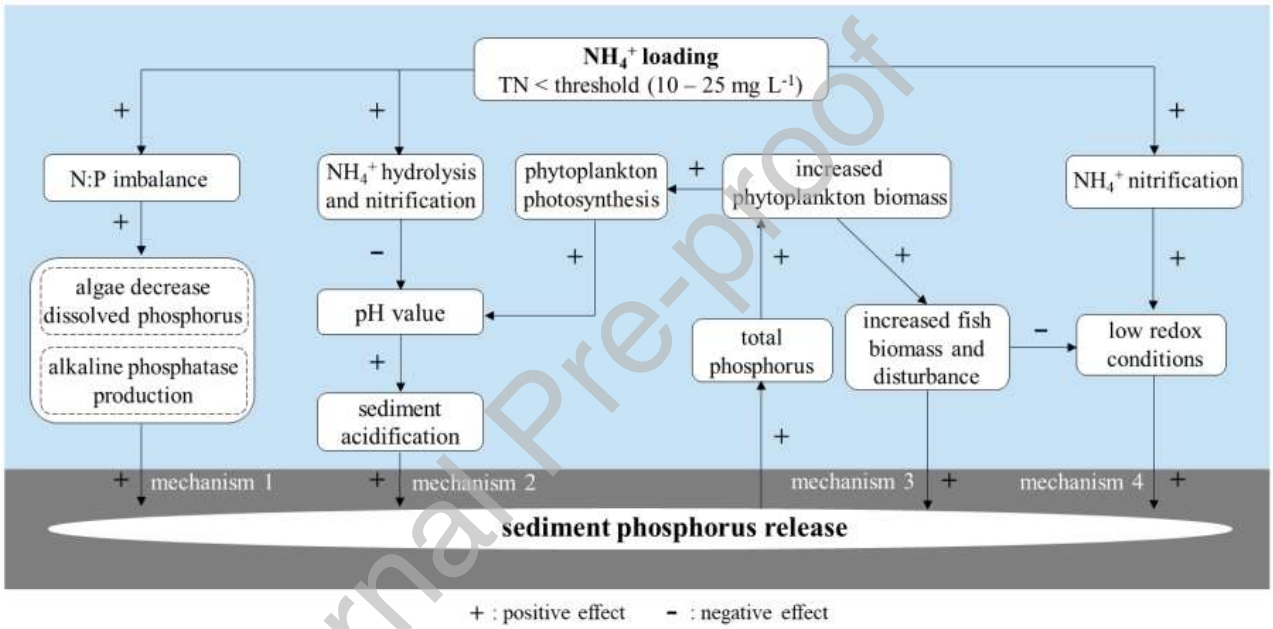

Fig. 8. Conceptual diagram depicting the processes and mechanisms of sediment phosphorus release in response to increased ammonium loading at long-term whole-ecosystem level.

Declaration of interests

☒ The authors declare that they have no known competing financial interests or personal relationships that could have appeared to influence the work reported in this paper.

☐ The authors declare the following financial interests/personal relationships which may be considered as potential competing interests: